

Nanoimprint of dehydrated PEDOT:PSS for organic photovoltaics

This article has been downloaded from IOPscience. Please scroll down to see the full text article.

2011 Nanotechnology 22 485301

(<http://iopscience.iop.org/0957-4484/22/48/485301>)

View [the table of contents for this issue](#), or go to the [journal homepage](#) for more

Download details:

IP Address: 129.110.5.91

The article was downloaded on 23/12/2011 at 21:51

Please note that [terms and conditions apply](#).

Nanoimprint of dehydrated PEDOT:PSS for organic photovoltaics

Y Yang¹, K Lee², K Mielczarek², W Hu^{1,3} and A Zakhidov^{1,2}

¹ Department of Materials Science and Engineering, University of Texas at Dallas, Richardson, TX 75080, USA

² Department of Physics, University of Texas at Dallas, Richardson, TX 75080, USA

³ Department of Electrical Engineering, University of Texas at Dallas, Richardson, TX 75080, USA

E-mail: walter.hu@utdallas.edu and zakhidov@utdallas.edu

Received 5 September 2011

Published 4 November 2011

Online at stacks.iop.org/Nano/22/485301

Abstract

We demonstrate the fabrication of poly(3,4-ethylenedioxythiophene) poly(styrenesulfonate) (PEDOT:PSS) nanogratings by a dehydration-assisted nanoimprint lithographic technique. Dehydration of PEDOT:PSS increases its cohesion to protect the nanostructures formed by nanoimprinting during demolding, resulting in the formation of high quality nanogratings of 60 nm in height, 70 nm in width and 70 nm in spacing (aspect ratio of 0.86). PEDOT:PSS nanogratings are used as hole transport and an electron blocking layer in blended poly(3-hexylthiophene-2,5-diyl) (P3HT):[6,6]-phenyl-C61-butyric-acid-methyl-ester (PCBM) organic photovoltaic devices (OPV), showing enhancement of photocurrent and power efficiency in comparison to OPV devices with non-patterned PEDOT:PSS films.

(Some figures may appear in colour only in the online journal)

1. Introduction

In recent years, research progress in organic photovoltaic (OPV) devices has advanced tremendously, driven by the potential for low cost, large area and flexible devices [1, 2]. However, one major challenge for OPV is its relatively low power conversion efficiency (PCE), compared to other types of inorganic solar cells and its commercialization potential is thus hindered [3–5]. One emerging method to improve PCE for OPV is nanoimprint lithography (NIL), which provides an ordered and continuously interdigitized morphology in active layers for both efficient charge separation and collection [6–8]. In addition, NIL can be used to pattern electrodes such as indium tin oxide (ITO) and Au in OPVs and a more efficient charge carrier collection was observed [9, 10]. Besides those inorganic electrodes, nanoimprinted poly(3,4-ethylenedioxythiophene) poly(styrenesulfonate) (PEDOT:PSS), a widely used organic anode material for OPV due to its high work function, transparency and conductivity is also of interest. However, due to its low cohesion and softness [11], the PEDOT:PSS structures formed by NIL are easy to destroy

during demolding. Previously reported PEDOT:PSS structures by nanoimprinting are limited to microscale structures with low aspect ratios ($AR \sim 10^{-2}$) [12]. Because of this patterning challenge, the application of imprinting PEDOT:PSS nanostructures for devices has been very limited.

In this paper, we report a new dehydration-assisted nanoimprint technique to overcome the above-mentioned material limitation to fabricate PEDOT:PSS nanogratings with higher aspect ratio. For the first time, a large scale of high quality PEDOT:PSS nanogratings with height $h = 60$ nm, width $w = 70$ nm and spacing $p = 70$ nm was achieved, which gave an aspect ratio of 0.86. Using this nanoimprinted PEDOT:PSS film as the hole transport/electron block layer (HTL/EBL), bulk heterojunction OPV of poly(3-hexylthiophene-2,5-diyl) (P3HT):[6,6]-phenyl-C61-butyric-acid-methyl-ester (PCBM) has shown an increase in PCE by 15% in comparison to the PCE of OPV devices using non-patterned PEDOT:PSS film. This nanoimprint-introduced efficiency increase is attributed to the increased PEDOT:PSS interfacial area, possibly better molecular chain alignment and enhanced charge carrier collection.

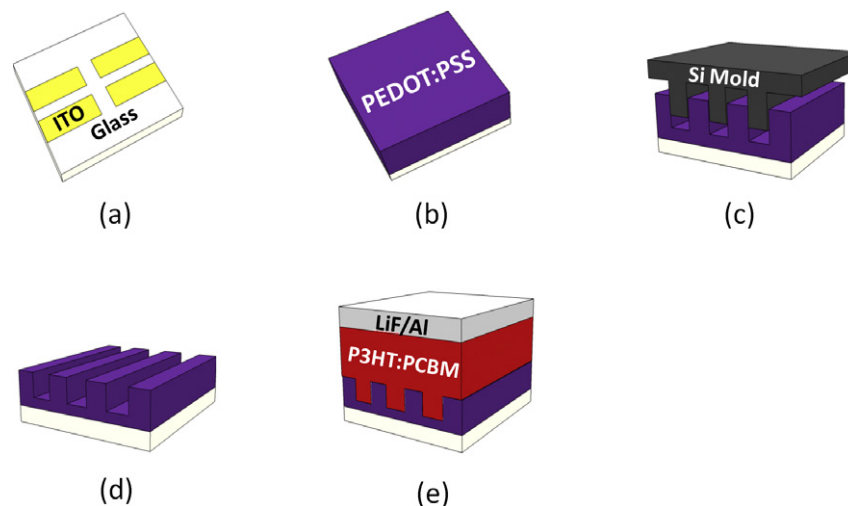


Figure 1. Schematic of (a) patterning ITO, (b) spin-coating PEDOT:PSS, (c) nanoimprinting, (d) creating PEDOT:PSS nanogratings and (e) spin-coating P3HT:PCBM and thermal evaporation of LiF and Al.

2. Experimental details

2.1. Nanoimprint of PEDOT:PSS nanogratings

In this work, low conductive PEDOT:PSS (CLEVIOS P VP Al 4083, H C Starck, Inc.) was chosen as HTL/EBL for organic solar cells to minimize the measurement error from device areas due to the lateral conductivity of PEDOT:PSS. A thin layer (~ 70 nm) of PEDOT:PSS was filtered with $0.45 \mu\text{m}$ PTFE filter and spin-coated onto substrates (ITO or Si), which was treated with ultraviolet ozone for 5 min. After being left in a desiccator with $\sim 15\%$ relative humidity (rH) for 24 h to dehydrate, PEDOT:PSS films were nanoimprinted using an Si nanograting mold with $h = 60$ nm, width $w = 70$ nm and spacing $p = 70$ nm at 100°C and 2 MPa for 600 s to form nanostructures. For comparison, PEDOT:PSS films were also spin-coated and imprinted in ambient air (with $\sim 45\%$ rH) without any dehydration as reference.

2.2. Solar cell fabrication and characterization

Solar cells were fabricated using nanoimprinted PEDOT:PSS films in the following structure of OPV: indium tin oxide (ITO)/PEDOT:PSS/P3HT:PCBM/LiF/Al and the general schematic of a fabrication flow is shown in figure 1. After spin-coating onto patterned ITO-coated glass substrates, which were treated with ultraviolet ozone for 5 min, PEDOT:PSS films were imprinted under the same conditions introduced above. Then, the nanoimprinted PEDOT:PSS films were spin-coated with a layer (~ 200 nm) of blended P3HT (Reike Metal, Ltd):PCBM (Nano-C) onto nanogratings from $1:1$ 20 mg ml^{-1} P3HT:PCBM solution in chlorobenzene mixed with 2.5% v/v 1,8-octanedithiol (ODT), which helps P3HT and PCBM phases separate into small domains without the need for additional thermal annealing [13]. Finally, 1 nm LiF and 100 nm Al were thermally evaporated on top as the cathode. Four solar cell pixels were formed on each substrate with an active area each of 9 mm^2 . It is worth noting that both temperature (via thermal annealing) and pressure

have shown negative impacts on PEDOT:PSS conductivity. For example, Dimitriev *et al* has shown the resistance of PEDOT:PSS increases with annealing temperature because thermal energy can disturb the molecular chain alignment in the molecules [14]. Also according to Lang *et al* PEDOT:PSS is a piezoresistive material [15]. Its molecular chain alignment can be disturbed under applied pressure and lead to higher resistance. Therefore to clarify the effects of imprint temperature, pressure and nanostructure morphology on the PEDOT:PSS properties and device performance, besides non-treated and imprinted devices, P3HT:PCBM solar cells were also made using PEDOT:PSS films pressed with a flat non-patterned Si mold under the same temperature of 100°C and pressure of 2 MPa and their combination for 600 s. After the OPV devices were made, their current density–voltage (J – V) characteristics were measured using Air Mass 1.5 global solar simulated light (AM. 1.5G) calibrated using an NREL traceable KG5 color-filtered silicon photodiode (PV Measurements Inc.) to an intensity of 100 mW cm^{-2} .

3. Results and discussion

The results of dehydration-assisted nanoimprinting are shown in figure 2 with the SEM image of the Si mold shown in figure 2(a). Figures 2(b) and (c) show the SEM images of the regularly imprinted in ambient air (with $\sim 45\%$ rH) and dehydration-assisted imprinted PEDOT:PSS nanogratings, respectively, representing a sharp difference. Because of the low cohesion in its molecules, PEDOT:PSS nanogratings formed by NIL without any dehydration treatment before were peeled off from the residual layer and serious deformation was observed everywhere (figure 2(b)). However, as shown in figure 2(c), after dehydration, high patterning fidelity and high quality of PEDOT:PSS nanostructures were enabled by the enhanced cohesion in the low rH environment. For the first time, large-scale PEDOT:PSS nanogratings ($2 \times 2 \text{ cm}^2$) with height $h = 60$ nm, width $w = 70$ nm and spacing $p = 70$ nm are duplicated from the Si mold, resulting in an

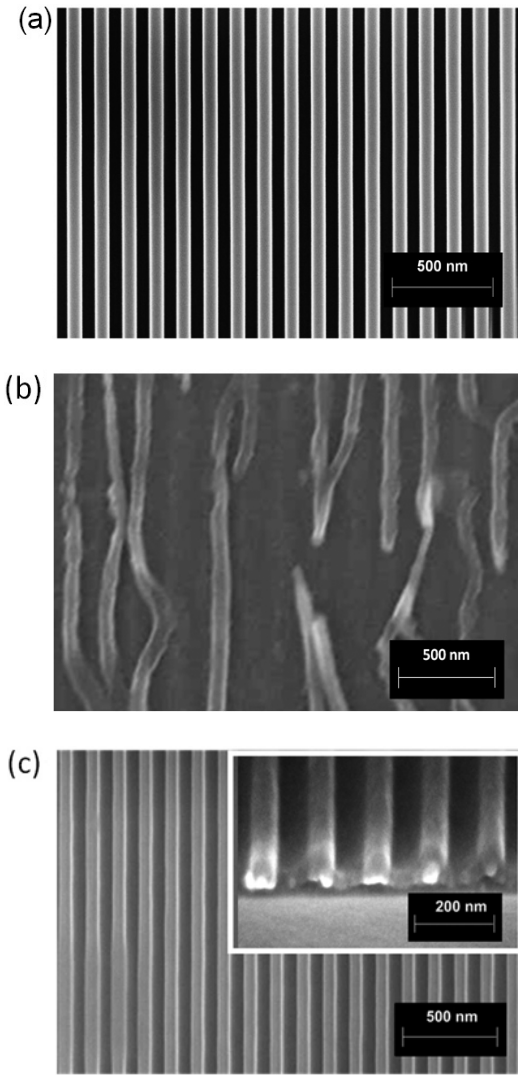


Figure 2. SEM images of (a) Si nanolined mold, nanoimprinted PEDOT:PSS nanogratings (b) without and (c) with dehydration.

AR of 0.86 ($h/w = 0.86$). This is a significant enhancement of PEDOT:PSS patterning in comparison to the previously reported work. Achieving high aspect ratio PEDOT:PSS nanostructures may enhance OPV performance. As shown in equation (1) the increase of surface area for charge collection by the imprinted PEDOT:PSS gratings can be quantified as the interface enhancement factor (IEF), which is 1.86 as compared to the planar PEDOT:PSS layer (IEF = 1) [16]. With such a large area of PEDOT:PSS nanogratings with high AR, it is possible to use it to make organic solar cells improve the hole collection:

$$\text{IEF} = 1 + \frac{2h}{w+p} = 1 + \frac{h}{w}, \quad \text{when } h = p. \quad (1)$$

An increase in AR for imprinted PEDOT:PSS nanostructures by dehydration can be explained in figure 3. During demolding, i.e. when the mold is being removed from PEDOT:PSS nanogratings with height h , width w and length l vertically, two energies are competing with each other. The first energy is the adhesion $W_{\text{mp}}^{\text{a}} = \gamma_{\text{mp}}$ at the interface between

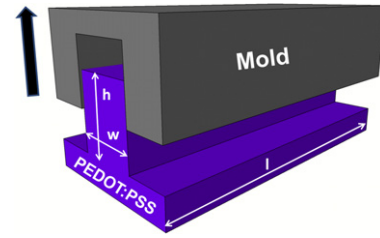


Figure 3. Demolding for nanoimprinted PEDOT:PSS nanograting.

the FDTS-treated mold and PEDOT:PSS nanostructures and defined by equation (2) [17, 18], where γ_{mp} is the interfacial surface energy in between, A_{mp} is the contact area and μ_{d} is dynamic friction. The other energy is the cohesion W_{p}^{c} within the polymer and defined by equation (3), where γ_{p} is the overall surface energy of the polymer, A_{p} is the cross-sectional area of each PEDOT:PSS nanograting and $\gamma_{\text{p}}^{\text{d}}$, $\gamma_{\text{p}}^{\text{p}}$, $\gamma_{\text{p}}^{\text{h}}$, etc. are its components due to dispersive forces, polar forces, hydrogen bonding forces, etc. respectively. The cohesion of the polymer is due to these forces. Lang *et al* have found that PEDOT:PSS molecules are made of PEDOT-rich cores wrapped in PSS-rich shells and its cohesion is by the hydrogen bonds in PSS-rich shells [11]. It indicates that, for PEDOT:PSS, W_{p}^{c} is mainly determined by $\gamma_{\text{p}}^{\text{h}}$, the hydrogen bonding surface energy, as concluded in equation (3). For successful demolding, adhesion must be less than cohesion ($W_{\text{mp}}^{\text{a}} = \gamma_{\text{mp}} < W_{\text{p}}^{\text{c}}$), otherwise the nanostructure can break. Therefore it can be concluded that the AR of nanostructures made by nanoimprinting is proportional to the ratio of $\gamma_{\text{p}}^{\text{h}}$ to γ_{mp} , as shown in equation (4). It has been shown that, in ambient air, the hydrophilic PSS-rich shell can absorb moisture in the air and swells the whole molecule [11]. The hydrogen bonds in PSS-rich shells are thus weakened by this swelling and lead to a low $\gamma_{\text{p}}^{\text{h}}$ for PEDOT:PSS, which makes it hard to fabricate high AR nanostructures. In this work, using dehydration to remove the moisture in PSS-rich shells, the cohesion for PEDOT:PSS molecules is increased due to the enhanced hydrogen bonds and a higher AR becomes possible.

$$W_{\text{mp}}^{\text{a}} = \gamma_{\text{mp}} A_{\text{mp}} = \gamma_{\text{mp}} [2\mu_{\text{d}}(hw + hl) + lw] \quad (2)$$

$$W_{\text{p}}^{\text{c}} = \gamma_{\text{p}} A_{\text{p}} = (\gamma_{\text{p}}^{\text{d}} + \gamma_{\text{p}}^{\text{p}} + \gamma_{\text{p}}^{\text{h}} \dots) lw \cong \gamma_{\text{p}}^{\text{h}} lw \quad (3)$$

$$\frac{h}{w} < 1 + \frac{1}{2\mu_{\text{d}}} \left(\frac{\gamma_{\text{p}}^{\text{h}}}{\gamma_{\text{mp}}} - 1 \right) - \frac{h}{l} \cong 1 + \frac{1}{2\mu_{\text{d}}} \left(\frac{\gamma_{\text{p}}^{\text{h}}}{\gamma_{\text{mp}}} - 1 \right), \quad \text{when } W_{\text{mp}}^{\text{a}} = \gamma_{\text{mp}} < W_{\text{p}}^{\text{c}}. \quad (4)$$

The J - V characteristics of these devices are shown in figure 4. Shunt resistance (R_{sh}), series resistance (R_{s}), open circuit voltage (V_{oc}), short circuit current (J_{sc}), fill factor (FF) and PCE of these devices are extracted from the J - V curves and listed in table 1. For each device with PEDOT:PSS differently treated, the results were calculated from the average of four OPV pixel devices on the same substrate and their standard deviations were calculated. We found that device performance is highly dependent on the PEDOT:PSS treatment conditions. Compared to a non-imprinted device (D1), those flat-imprinted at 100 °C (D2) show similar R_{sh} but increased R_{s} , leading to a similar V_{oc} but decreased J_{sc} and FF, a relation well observed in others' work [19, 20]. Although high

Table 1. Performance of P3HT:PCBM solar cells with PEDOT:PSS non-imprinted (D1), imprinted by plain Si mold at 100 °C (D2), imprinted by plain Si mold at 2 MPa (D3), imprinted by plain Si mold at 100 °C and 2 MPa (D4) and imprinted by nanolined Si mold at 100 °C and 2 MPa (D5).

Device	D1	D2	D3	D4	D5
R_{sh} (M Ω)	8.82 ± 0.21	9.18 ± 0.26	9.70 ± 0.20	9.12 ± 0.18	9.04 ± 0.19
R_s (Ω)	44.86 ± 0.25	63.17 ± 0.94	54.96 ± 0.21	80.92 ± 0.26	36.78 ± 0.15
V_{oc} (V)	0.55 ± 0.0001	0.55 ± 0.0001	0.56 ± 0.0005	0.55 ± 0.0001	0.57 ± 0.0001
J_{sc} (mA cm $^{-2}$)	8.13 ± 0.12	7.15 ± 0.08	7.70 ± 0.09	5.06 ± 0.04	8.27 ± 0.02
FF	0.54 ± 0.01	0.48 ± 0.01	0.50 ± 0.02	0.18 ± 0.02	0.59 ± 0.01
η (%)	2.44 ± 0.03	1.91 ± 0.04	2.14 ± 0.04	0.50 ± 0.01	2.80 ± 0.02

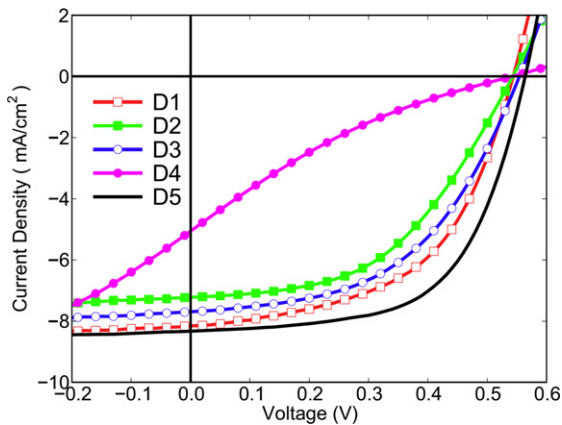


Figure 4. J - V characteristics of P3HT:PCBM solar cells with PEDOT:PSS non-imprinted (D1), imprinted by plain Si mold at 100 °C (D2), imprinted by plain Si mold at 2 MPa (D3), imprinted by plain Si mold at 100 °C and 2 MPa (D4) and imprinted by nanolined Si mold at 100 °C and 2 MPa (D5).

temperatures over 100 °C are typically used in other people's work to drive off moisture in PEDOT:PSS and do not affect the solar cell performance [3, 5, 19, 20], our devices show a high sensitivity to temperature. The reason for this controversial observation can be because in our imprinting process a relatively thick (70 nm) and low conductive PEDOT:PSS (up to 5000 Ω cm according to H C Starck, Inc.) is used in order to minimize measurement errors. Thus the contribution of this thick and low conductive HTL/EBL to the overall R_s of the device is not negligible and makes device performance highly dependent on its resistance, which is affected by treatment temperatures. A similar decrease is also observed for those flat-imprinted devices at 2 MPa and room temperature (D3) but to a lesser degree. Devices which were flat-imprinted at both 100 °C and 2 MPa (D4) show the highest R_s and thus the lowest J_{sc} and FF. This is due to the synergic disturbing effects on chain alignment when high temperature and pressure are applied together, which significantly reduced the device PCE. However, interestingly, the solar cells built on imprinted PEDOT:PSS nanogratings (D5) at the same 100 °C and 2 MPa show similar R_{sh} but the lowest R_s , resulting in the highest J_{sc} and FF. A 15% increase in PCE over the non-imprinted planar device (D1) is observed. In this work, though small standard deviations were demonstrated from each type of device as shown in table 1, to further reduce the experimental errors, we remade three batches of P3HT:PCBM solar cells with PEDOT:PSS treated under the

same differences. Similar trends were observed for each kind of device. Therefore, we believe there must be other factors in the PEDOT:PSS nanogratings besides the increased interfacial area to overcome the significantly negative effects of high temperature and pressure on PEDOT:PSS film resistance. Most likely, this is because NIL with nanostructured mold induces better polymeric chain alignment during the formation of nanogratings, which has been observed in P3HT nanogratings by XRD as shown in our previous work [21]. Ordered chain alignment in nanogratings, which takes place during the vertical upwards flow of polymeric matter into openings of the nanomold, would reduce R_s and improve PCE via increased J_{sc} and FF. Another possible mechanism is that PEDOT:PSS nanogratings might change the directions of the electric field in the active layer and make the holes dissociated close to the cathode able to be collected by shortening the hole collection path. These holes are hard to collect in non-imprinted devices due to the relatively short hole drift length. A schematic overview of the proposed mechanisms is shown in figure 5. The device performance shows that the positive effect of imprinted PEDOT:PSS nanostructures is dominant over the negative effects of high temperature and pressure. Currently NIL is mainly used to pattern organic active layer materials (particularly the P3HT donor component) to improve the OPV efficiency [8, 22–24], but our work shows that application of this technique to PEDOT:PSS, a widely used HTL/EBL material, can also increase the solar cell performance. Although PEDOT:PSS only acts to transport holes (and block electrons) in bulk heterojunction OPV and does not itself generate additional charge carriers, we still observe a 15% increase in PCE with an enhanced interface (1.86 IEF), even on account of those negative effects from high imprint temperature and pressure.

The relative PCE improvement in devices using PEDOT:PSS nanogratings over those using a planar non-imprinted PEDOT:PSS film proves that NIL of HTL/EBL is a promising method to increase the performance of organic solar cells. We believe a higher PCE can be expected by further optimization. Besides optimizing the P3HT:PCBM active layer, such as P3HT:PCBM ratios, solution concentrations and active layer thicknesses to have an overall PCE increase, it is also possible to obtain a higher performance by decreasing the PEDOT:PSS residual layer thickness to better transmit light and transport holes or dehydrating PEDOT:PSS in an oxygen- and moisture-free environment to prevent possible polymer degradation during dehydration. The device PCE might also be further increased with higher IEF by increasing grating height

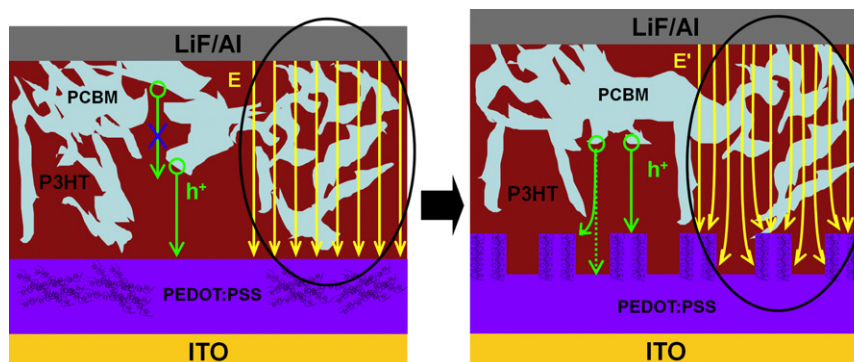


Figure 5. Comprehensive schematic overview of the proposed mechanisms: nanoimprint might introduce molecular chain alignment in PEDOT:PSS nanogratings and decrease the PEDOT:PSS resistance. Also the change of direction of the electric field from E in a device using non-imprinted PEDOT:PSS film to E' in a device using PEDOT:PSS nanogratings makes the holes (h^+) dissociated close to the cathode able to be collected by shortening the hole collection path from dashed line to solid line. These holes are supposed to recombine with electrons in non-imprinted devices due to the relatively short hole drift length.

and reducing grating pitch. Creating PEDOT:PSS nanogratings at lower temperature and pressure is expected to also further increase the PCE by reducing synergistic negative effects of temperature and pressure. These PEDOT:PSS nanogratings may also find applications in organic transistors and light-emitting diodes.

4. Conclusions

In summary, we conclude that dehydration-assisted nanoimprint lithography is an effective way to pattern high quality and high density PEDOT:PSS nanogratings with high aspect ratio over a large scale. Dehydration increases the cohesion of PEDOT:PSS molecules to prevent the nanogratings formed by NIL from breaking during demolding. P3HT:PCBM organic solar cells using these PEDOT:PSS nanogratings as the hole collection layer show improved PCE and it can be attributed to the enhanced hole collection efficiency.

Acknowledgments

This work is supported by the National Science Foundation (no. ECCS-0901759), Welch Foundation grant AT-1617, DOE STTR grant and Rice/AFRL grant of CONTACT/AF consortium of Texas. The authors gratefully acknowledge Suresh Regonda from the Physics Department at UT Dallas for his support and helpful discussions.

References

- [1] Lewis N S 2007 *Science* **315** 798
- [2] Tong S W, Zhang C F, Jiang C Y, Liu G, Ling Q D, Kang E T, Chan D S H and Zhu C X 2008 *Chem. Phys. Lett.* **453** 73
- [3] Park S H, Roy A, Beaupré S, Cho S, Coates N, Moon J S, Moses D, Leclerc M, Lee K and Heeger A J 2009 *Nature Photon.* **3** 297
- [4] Martin A G, Keith E, Yoshihiro H and Wilhelm W 2009 *Prog. Photovolt. Res. Appl.* **17** 320
- [5] Liang Y, Xu Z, Xia J, Tsai S, Wu Y, Li G, Ray C and Yu L 2010 *Adv. Mater.* **22** 1
- [6] Dissanayake D M N M, Adikaari A A D T and Silva S R P 2008 *Appl. Phys. Lett.* **92** 093308
- [7] Nanditha D M, Dissanayake M, Hatton R A, Curry R J and Silva S R P 2007 *Appl. Phys. Lett.* **90** 113505
- [8] Aryal M, Buyukserin F, Mielczarek K, Zhao X M, Gao J M, Zakhidov A and Hu W 2008 *J. Vac. Sci. Technol. B* **26** 2562
- [9] Yang K, Lim K Y S and Lee H 2009 *J. Vac. Sci. Technol. B* **27** 2786
- [10] Kang M, Kim M, Kim J and Guo L 2008 *Adv. Mater.* **20** 4408
- [11] Lang U, Naujoks N and Dual J 2009 *Synth. Met.* **159** 473
- [12] Emah J B, Curry R J and Silva S R P 2008 *Appl. Phys. Lett.* **93** 103301
- [13] Lee J K, Wan L M and Brabec C 2008 *J. Am. Chem. Soc.* **130** 3619
- [14] Dimitriev O P, Grinko D A, Noskov Yu V, Ogurtsov N A and Pud A A 2009 *Synth. Met.* **159** 2237
- [15] Lang U, Rust P, Schoberle B and Dual J 2009 *Microelectron. Eng.* **86** 330
- [16] Yang Y, Aryal M, Mielczarek K, Hu W and Zakhidov A 2010 *J. Vac. Sci. Technol. B* **28** C6M104
- [17] Owens D K and Wendt R C 1969 *J. Appl. Polym. Sci.* **13** 1741
- [18] Tao L, Zhao X, Gao J and Hu W 2010 *Nanotechnology* **21** 095301
- [19] Ma W, Yang C, Gong X, Lee K and Heeger A J 2005 *Adv. Funct. Mater.* **15** 1617
- [20] Li G, Shrotriya V, Huang J, Yao Y, Moriarty T, Emery K and Yang Y 2005 *Nature Mater.* **4** 864
- [21] Aryal M, Trivedi K and Hu W 2009 *ACS Nano* **3** 3085
- [22] Wiedemann W et al 2010 *Appl. Phys. Lett.* **96** 263109
- [23] Cheyins D, Vasseur K, Rolin C, Genoe J, Poortmans J and Heremans P 2008 *Nanotechnology* **19** 424016
- [24] Shih C F, Hung K T, Wu J W, Hsiao C Y and Li W M 2009 *Appl. Phys. Lett.* **94** 143505